Vol 17 No 2, February 2008
1674-1056/2008/17(02)/0637-07

Chinese Physics B

© 2008 Chin. Phys. Soc.
and IOP Publishing Ltd

Correlation dimension analysis and capillary wave turbulence in Dragon-Wash phenomena*

Peng Huai-Wu(彭怀午), Li Rui-Qu(李睿劬),
Chen Song-Ze(陈松泽), and Li Cun-Biao(李存标)†

State Key Laboratory for Turbulence and Complex Systems
Department of Mechanics and Aerospace Engineering,
College of Engineering, Peking University, Beijing 100871, *China*

(Received 15 March 2007; revised manuscript received 20 August 2007)

This paper describes the evolution of surface capillary waves of deep water excited by gradually increasing the lateral external force at a single frequency. The vertical velocities of the water surface are measured by using a Polytec Laser Vibrometer with a thin layer of aluminium powder scattering on the surface to reflect the laser beam. Nonlinear interaction processes result in a stationary Fourier spectrum of the vertical surface velocities (the same as the surface elevation), i.e. $I_\omega \sim \omega^{-3.5}$. The observed spectrum can be interpreted as a wave-turbulent Kolmogorov spectrum for the case of 'narrowband pumping' for a direct cascade of energy. Correlation dimension analysis of the whole development process reveals four distinct stages during the wave structure development and identifies the wave turbulence stage.

Keywords: capillary wave, wave turbulence, correlation dimension
PACC: 4735, 9210H, 9210L

1. Introduction

In this paper we describe laterally excited surface waves that are similar to the Faraday waves, in a cylindrical container, motivated by the Chinese ancient cultural relic 'Dragon-Wash'. Wang[1,2] first studied the Dragon-Wash phenomenon and found that a high frequency external excitation could produce a low frequency gravity wave, which was similar to the spatial resonance phenomenon observed by Huntley.[3] Mahony and Smith[4] proposed that the nonlinear coupling between two modes by modal decomposition resulted in low frequency standing surface waves. Hsieh[5,6] offered the same idea that the mechanism for the generation of low-frequency gravity waves was the mode-mode interaction. Various theoretical studies on the surface waves related to the Dragon-Wash phenomenon have also been carried out by Shen and Hsieh,[7] Hsieh,[8] and Sun *et al.*[9] Further experiments have been done by Wei *et al*[10] to measure the flow field by using the particle image velocimetry (PIV) technique and by Hsieh and Denissenko[11] to take photographs of the low amplitude surface waves by using the shadowgraph method. Figure 1 is a typical image of surface waves in Dragon-Wash phenomenon, which illustrates circumferential secondary waves and four potential droplet ejection regions.

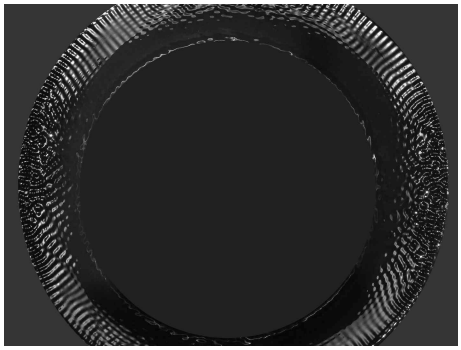


Fig.1. Photograph of capillary 'secondary' waves and four potential jumping droplet regions. Secondary waves are the most important part in the experiments with the development of secondary waves resulting from intense interactions between the surface waves.

Wave turbulence in Dragon-Wash phenomenon is an important part of the present paper. Wave turbulence theory was first proposed by Zakharov and Filonenko[12,13] forty years ago. Meanwhile, Benney and Saffman[14] derived a closed equation for the energy spectrum function of random, dispersive waves with weak nonlinear interactions, without assuming

*Project supported by the National Natural Science Foundation of China (Grant No 10087101) and the National Science Fund for Distinguished Young Scholars (Grant No 10525208).
†Corresponding author. E-mail: cblee@mech.pku.edu.cn

Gaussian distribution of the waves. Later on, Newell *et al*[15] reviewed the wave turbulence in collection with the phenomenon of intermittency and emphasized the key roles of finite flux solutions in non-equilibrium systems. The Kolmogorov solution is an exact solution of the Hasselman–Zakharov kinetic equation[16] for the stationary case. For gravity surface waves, the pioneering work by Toba[17] and the one-dimensional spectrum obtained by Hwang *et al*[18] using an airborne scanning lidar system were in good agreement with wave turbulence theory.

In the present study, nonlinear capillary waves on a water surface are investigated for the flow in a turbulent regime. The capillary waves on the surface of a liquid are known to represent an example of nonlinearly interacting waves characterized by the dissipation of energy mainly at high frequencies due to viscous losses. The dispersion law of capillary waves is of decay type, the wave frequency $\omega_k \sim k^{3/2}$, where k is the wave number. Therefore, the resonance of the three-wave interaction will dominate the dynamics. The theory of homogeneous capillary turbulence was described by Zakharov and Filonenko.[13] They found a surface-height spectrum with a frequency representation, $I_\omega = \left\langle |\eta_\omega|^2 \right\rangle = \text{const}\ \omega^{-17/6}$, where $\eta(r,t)$ is the surface elevation.

The case of single resonance frequency pumping was described by the experimental result of Brazhinkov *et al*[19] which showed that the frequency dependence of the peak height was an exponential function with an exponent close to –3.5, which was the result calculated by Fal'kovich and Shafarenko[20] for the case of 'narrowband pumping', i.e. $I_\omega \sim \omega^{-3.5}$. The power dependence on the frequency for the surface-height spectrum of the capillary waves in a wave turbulent regime was also observed in experiments on water by Wright *et al*[21,22] with the exponent of the power function being –3.2, and it was also found by Henry *et al*[23] through using the diffusing light technique and by Brazhnikov *et al*[24] in terms of laser beam reflection to a photo-detector. Westra[25] used low-viscosity and low surface tension silicon oil as a fluid in experiment and obtained an exponent –3.6 ± 0.1 by using the laser refraction method. Brazhnikov *et al*[19,26–28] also observed the turbulence of the capillary waves on the surface of liquid hydrogen and found that the exponent of the power function was equal to –3.7 ± 0.3, when the surface was excited at the resonance frequency. One problem in these experiments was that it was hard to assess the linearity of their measurement techniques. We used a completely new Polytec Scanning Vibrometer, which represented the state-of-the-art measurement technology for the analysis of structural vibrations, to accurately measure the vertical velocities of the water surface.

The present paper concentrates on the wave evolution and the wave turbulence regime by measuring the time series of the vertical velocities on the free surface. Chaotic analysis is used to reconstruct the phrase traces from locally sampled time series, to measure the dimension change with increasing excitation acceleration and to identify the four distinct physical stages, including the wave turbulence stage.

2. Experimental method

The experiments were performed in the State Key Laboratory for Turbulence and Complex systems. The experimental apparatus had a glass cylindrical container with a 210 mm inner diameter and a 220 mm high and 3 mm thick upright side wall, which imitates the Dragon-Wash. The container was filled with 160 mm deep water. The wall was excited by exerting lateral vibrations at one point, with the basin bottom fixed by two blocks. The experimental setup is shown in Fig.2. A Polytec laser vibrometer was used to measure the vertical velocities on the water surface. The sample frequency was 2048 Hz with a sample time of 2 S for each point in the radial direction on the water surface. The excitation frequency was fixed at 156 Hz and the excitation force was given by the wall acceleration. Table 1 lists eleven different accelerations used in our experiment.

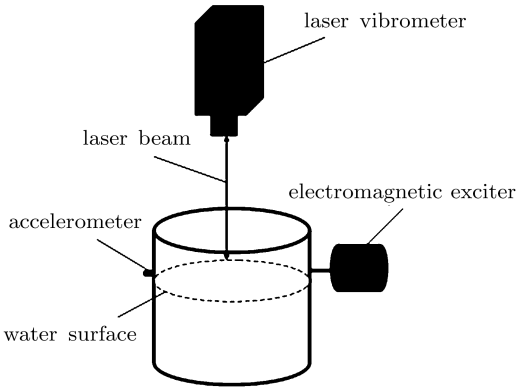


Fig.2. Experimental setup: a cylindrical container with an inner diameter of 210 mm was mounted on a frame and laterally vibrated by an electromagnetic exciter with a sinusoidal signal coming from a frequency synthesizer connected to a power amplifier.

Table 1. Eleven different excitation accelerations from a to $k(\mathrm{m/s^2})$ all with a frequency of 156 Hz.

case	a	b	c	d	e	f
acceleration	4.8	13.6	24.6	38	56	76
case	g	h	i	j	k	
acceleration	94	106	120	145	170	

3. Experimental results

The wave evolution process can be divided into four stages: a linear stage, a weakly nonlinear stage, a wave turbulence stage and low frequency gravity wave stage, as the driving acceleration increases. Detailed dynamic descriptions were given earlier,[29] so only a brief introduction is given here.

To visualize the attractor, phase portraits were constructed by embedding the trajectories in an m-dimensional phase space as suggested by Packard *et al*[30] and Takens,[31] which was found to be useful in other experiments.[32] The phase-space coordinates are $\{V(t), V(t+T), \ldots V(t+(m-1)T\}$, where T is the delay time. The phase portraits constructed in this way generally have the same dynamic properties as those constructed from a set of more logically chosen independent variables.[33] The embedding method depends on the fact that in a nonlinear system all variables are effectively coupled.

To calculate the correlation dimension, a correlation integral $C(r)$ is defined as the probability with which a pair of points chosen randomly with respect to the natural measure is separated by a distance less than r in the reconstructed phase space of m dimensions. The correlation integral $C(r)$ is then approximated by

$$C(N,r) = \frac{2}{N(N-1)} \sum_{j=1}^{N} \sum_{i=j+1}^{N} \theta(r - \| x_i - x_j \|),$$

where θ is the Heaviside function [$\theta(x) = 1$ for $x > 0$ and $\theta(x) = 0$ for $x \leq 0$] and $||\cdot||$ denotes a suitable vector norm. The correlation dimension D_2[33] of the attractor is then defined asymptotically as

$$D_2 = \lim_{r \to 0} \log C(r) / \log r.$$

3.1. Linear stage

When the external excitation amplitude is very small, axisymmetric circle capillary waves appear on the surface.[11,29,34] Their amplitudes are too small to be seen by the naked eyes, but the laser beam can easily capture the regular motion. Their amplitudes increase steadily with increasing external excitation acceleration. The phase portraits for cases (a)–(c) are limit cycles and the correlation dimensions are approximately unity. These phase portraits are not perfect limit cycles, due to the intrinsic dynamical or external noise.

In large containers (the inner diameter of the container in the present experiments is 210 mm), the lateral sinusoidal forcing is strong enough to overcome boundary effects. Basic equations for small amplitude waves are derived for the lateral excitation system, and the axisymmetric mode capillary waves are obtained without considering the meniscus effects in the work by Hsieh[6] and Peng *et al.*[29] Therefore, they are not induced mainly by meniscus effects, but they are easily excited by the high frequency lateral forcing, which is different from the vertically forced Faraday waves.

3.2. Weakly nonlinear stage

Further increasing the excitation amplitude results in the appearance of another kind of waves, which propagate in the circumferential direction.[11,29,34] The frequencies of these 'secondary' waves are almost half that of the 'primary' waves as shown in Fig.3. The wave interactions are intense and lead to the more complicated phase portrait and higher correlation dimension as shown in Figs.4 and 5. Two dimensions are clearly inadequate because the trajectories cross. Hence, three-dimensional phase portraits are constructed.

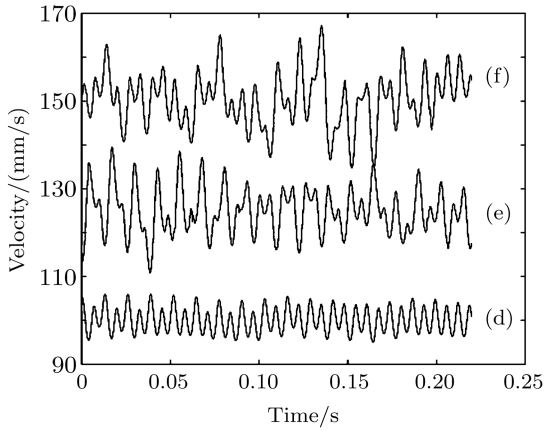


Fig.3. Time series of the vertical velocities in the nonlinear stage for an excitation frequency of 156.0 Hz and three different driving accelerations from d to f at the same point on the water surface.

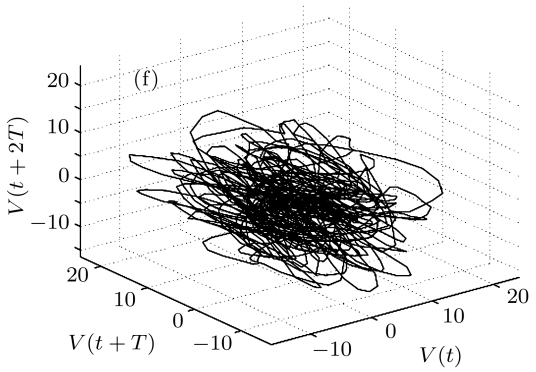


Fig.4. Phase portrait for case (f). The phase portraits for cases (d–f) are all more complicated than limit cycles. Two dimensions are clearly inadequate because the trajectories cross; therefore, three-dimensional phase portraits are used.

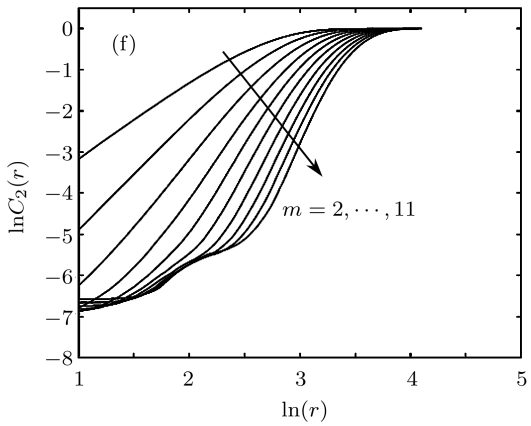


Fig.5. Sequence of correlation integrals for case (f) as $\ln C_2(r)$ vs $\ln(r)$ plots for a sequence of embedding dimensions $m = 2 \ldots 11$ from left to right. The limiting slope for large m is the correlation dimension of the attractor. Cases (d) and (e) are similar to case (f).

3.3. Wave turbulence stage

At higher excitation amplitudes, water droplets start to jump from the edge of the container.[11,29,34] The three-dimensional phase portraits can no longer be constructed because the correlation dimensions are higher than three.

The frequency dependence of the capillary waves was measured by using the Polytec laser vibrometer. The signals for the vertical velocities and wall accelerations were digitized at 20000 Hz by using a 12 bit A/D card with a sample time of 60 seconds. A typical vertical velocity signal for a forcing frequency of 162.7 Hz and wall acceleration of 86 m/s^2 is shown in Fig.6(a).

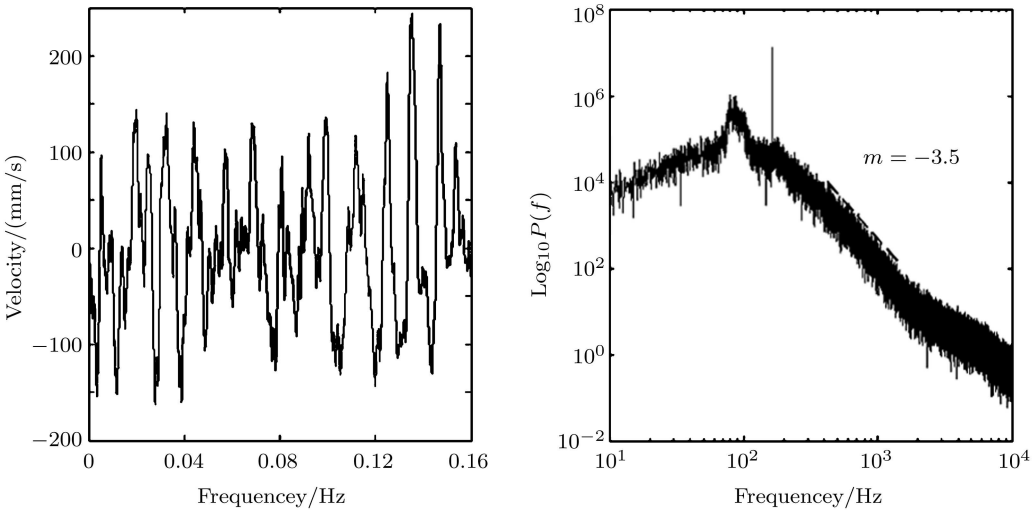


Fig.6. The vertical surface velocity trace and the corresponding power spectrum in the wave turbulence stage, showing (a) part of the time dependent vertical surface velocity trace for a high excitation of 86 m/s^2 and excitation frequency of 162.7 Hz and (b) power spectrum for wall excitation of 86 m/s^2 and excitation frequency of 162.7 Hz, where the dashed line indicates an exponent of –3.5.

The power spectrum for the exciting frequency of 162.7 Hz and wall accelerations of 86 m/s^2 is shown in Fig.6(b) by averaging over six measurements. The first peak in a frequency range of 0–100 Hz corresponds to the first half of harmonic excited by the external force. Between 100 and 200 Hz, the peak is at the excitation frequency. At frequencies above 200 Hz, the peak heights decrease monotonically on the average. In a frequency range of 200–1000 Hz, the power dependence is well described by a power function. For

comparison, the dashed line in the figure indicates the exponent –3.5, which is the theoretical value for the case of 'narrowband pumping'.[20]

Further experiments were carried out with different forcing frequencies to validate the wave turbulence theory. Typical vertical velocity signals for forcing frequencies of 155 Hz, 158 Hz and 160 Hz are shown in Figs.7(a), (c), and (e), respectively; and the power spectra by averaging over six measurements for forcing frequencies of 155 Hz, 158 Hz and 160 Hz are shown in Figs.7(b), (d), and (f), respectively. Therefore, similar results are obtained with different forcing frequencies, which further strengthens the agreement between the experiment and the wave turbulence theory.

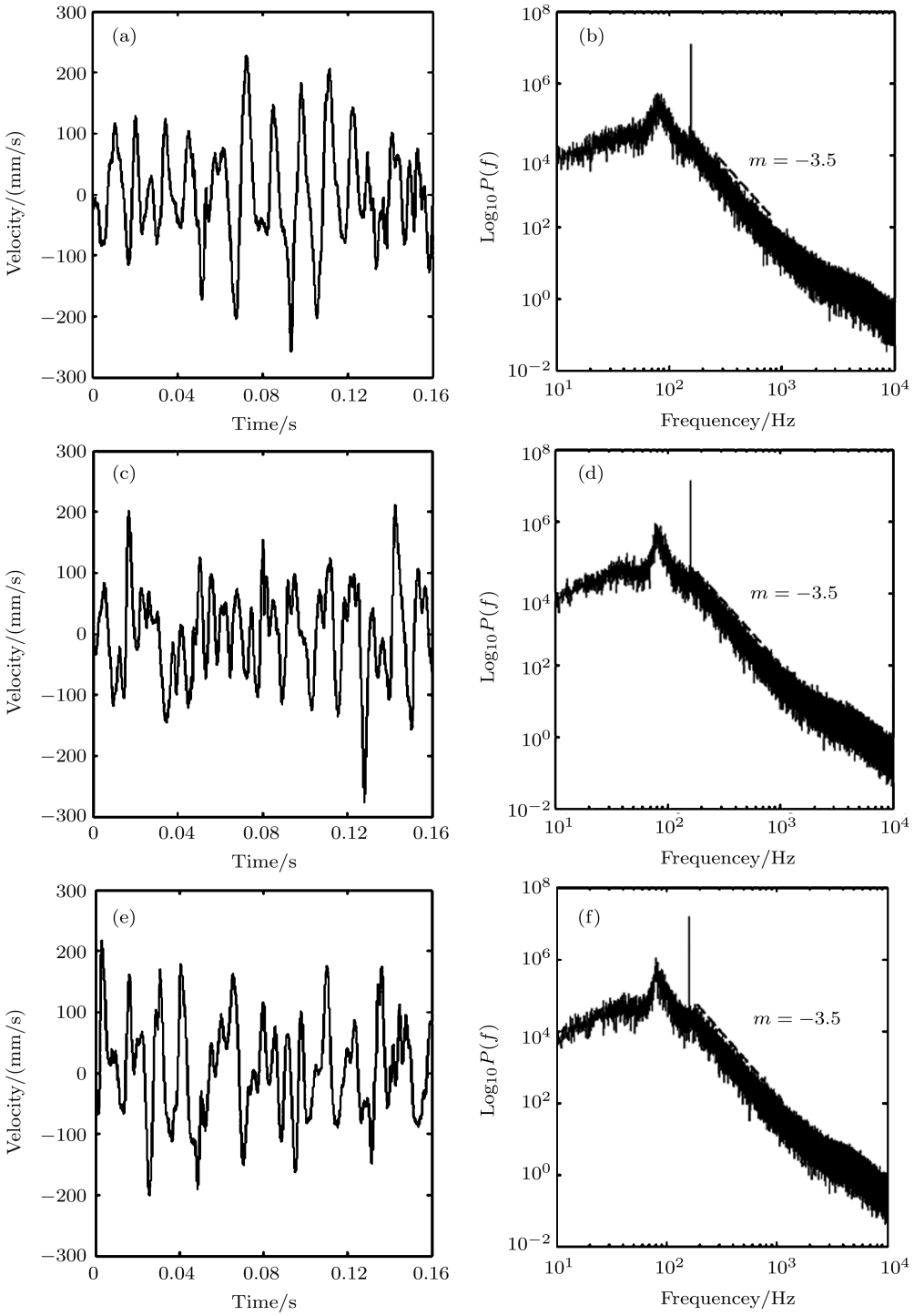


Fig.7. Typical vertical velocity signals for forcing frequencies of 155 Hz, 158 Hz and 160 Hz are shown in subfigures (a), (c), and (e), respectively; the power spectra by averaging over six measurements for the forcing frequency of 155 Hz, 158 Hz and 160 Hz are indicated in subfigures (b), (d), and (f), respectively, where the dashed line indicates an exponent of –3.5.

3.4. Low frequency gravity wave emerging stage

With further increasing the excitation amplitude, large amplitude gravity waves were observed[11,29,34] with high frequency capillary waves and jumping droplets still apparent.

The transition from the drop ejection regime to the gravity wave regime is intriguing and complex. The modulation instability of nonlinearly interacting surface waves is a possible physical mechanism for the appearance of the large amplitude gravity wave like the nonlinear formation of 'freak' waves in the ocean, which will be investigated more in further research. Wave breaking and other dissipation effects appear to be responsible for the modulation instability,[35] so the droplets ejection is also one of the candidates that trigger the transition. The characteristic frequency of the gravity wave is related to the mode of the gravity wave, the inner diameter of the container and the water depth. Actually, the shape of the gravity wave satisfies a Bessel function and the frequency of the gravity wave can be calculated from the dispersion relation, which has been done in the work by Hsieh[5] and Peng *et al.*[34]

Meanwhile, the transition from the drop ejection regime to the gravity wave regime is required to satisfy two conditions, i.e. the low frequency of the gravity wave should be comparable with the resonance bandwidth of the high-frequency response of the container-fluid system[3,4,36] and the excitation amplitude should be large enough to exceed a critical threshold. In experiment, the easiest way to excite the gravity waves was to set the excitation frequency to be $f_{\rm n} + f_{\rm g}$, where $f_{\rm n}$ is the natural frequency of the container and fluid system and $f_{\rm g}$ is the natural frequency of the emerging gravity wave.

3.5. Complete correlation dimension

As illustrated in Fig.8, the correlation dimension for the periodic oscillations at the lower driving accelerations are approximately unity (part A), which corresponds to the linear stage with the axisymmetric capillary waves in experiment. Above the subharmonic bifurcation, the correlation dimension sharply increases in the second stage (part B) which corresponds to the occurrence of secondary waves and the intense wave interactions seen in experiment. At higher excitation accelerations, water droplets start to jump from the edge of the container in experiment, which is the third stage (part C) where the correlation dimension increases slowly to a maximum and the surface waves reach a wave turbulence state. At larger accelerations, a large amplitude standing gravity wave is observed in experiment, which is the last stage (part D) where the correlation dimension decreases some with the occurring of the large wave structure.

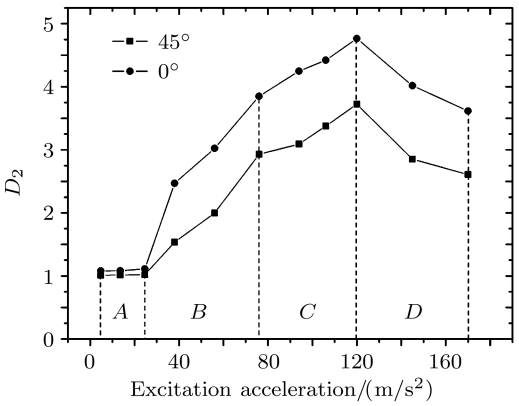


Fig.8. Correlation dimensions for various driving accelerations at the two different measured points showing the four stages for the four different physical processes: axisymmetric capillary waves, circumferential waves, jumping droplets, and gravity waves. 0° represents the measured point in the droplet ejection region, while 45° represents the measured point in the region where the droplets ejection region rotates 45° around the centre of the container.

The correlation dimension value of 0° curve is larger than that of the 45° curve with the development of the secondary waves, because the surface waves in the droplet ejection region are more chaotic. Time series of vertical velocities at many points on the free surface at different excitation accelerations were analysed by correlation dimension and spectrum approaches. It is found that, wave turbulence only occurs in highly chaotic droplet ejection regions where correlation dimensions correspond to larger values (larger than 3). The correlation dimensions for the different excitation frequencies have almost the same values, when the wave turbulence appears.

4. Discussion and conclusions

What is the physical mechanism for the transition to wave turbulence? Wu[37] showed that interactions between vortices could cause an instability of the surface shear layer and result in a transition to turbulence. This process is inherently viscous, though the

viscosity of the fluid may be small. As described by Lee,[38−40] the high shear layer and the vortical structures always appear along the borders of the waves where the velocity gradient is large and the viscous effects cannot be neglected.

Phase portraits allow the attractors to be visualized. The correlation dimensions demonstrate that the development of the secondary waves leads to a significant increase of fractional dimension. With the occurrence of jumping droplets, the dimension reaches the highest value, which just corresponds to the wave turbulence stage, while after the appearance of a low frequency gravity wave, the dimension deceases a little.

In the present work, a time series of the vertical velocities is used to analyse the nonlinear dynamics of the surface waves in a lateral oscillating fluid layer. The wave structure appears after the wave has experienced the developing process from periodic capillary waves to secondary waves to chaotic jumping droplets and to a large amplitude gravity wave with the excitation acceleration increasing in experiment,[11,29,34] which correspond to the four stages in Fig.8. The exponent of the power function for the single frequency excitation in these experiments is very close to –3.5, in excellent agreement with the theoretical value of wave turbulence for 'narrowband pumping'.[20]

Acknowledgments

The authors express their sincere thanks to Gregory Falkovich and D. J. Wang for valuable discussion. The authors are also grateful to H. J. Zhong for his help in preparing the experiment.

References

[1] Wang D J 1993 *Sci. Conservation and Archaeology* **5** 35
[2] Wang D J 2005 *Technische Mechanik* **25** 9
[3] Huntley I 1972 *J. Fluid Mech.* **53** 209
[4] Mahony J J and Smith R 1972 *J. Fluid Mech.* **53** 193
[5] Hsieh D Y 1997 *Acta Mech. Sin.* **13** 289
[6] Hsieh D Y 2000 *Acta Mech. Sin.* **16** 97
[7] Shen M C and Hsieh D Y 1993 *Wave Motion* **18** 401
[8] Hsieh D Y 1994 *Proc. Int. Conf. Hydrodynamics* (Beijing: China Ocean Press) p74
[9] Sun S M, Shen M C and Hsieh D Y 1995 *Wave Motion* **21** 331
[10] Wei Q, Wang D, Yan B, Du X and Chen J 1997 *Atlas of Visualization* III (New York: CRC Press) p169
[11] Hsieh D Y and Denissenko P 1998 *Tech. Rep.* 98-6-1, *Dept. Math.* (Hong Kong University of Science and Technology)
[12] Zakharov V E and Filonenko N N 1966 *Sov. Phys. Dokl* **11** 881
[13] Zakharov V E and Filonenko N N 1967 *J. Appl. Mech. Tech. Phys.* **4** 506
[14] Benney D J and Saffman P G 1966 *Proc. R. Soc. London, Ser.* A **289** 301
[15] Newell A C, Nazarenko S and Biven L 2001 *Physica* D **152-153** 520
[16] Zakharov V E, Falkovich G and Lvov V S 1992 *Kolmogorov Spectra of Turbulence,* Vol. 1: *Wave Turbulence* (Springer: Berlin) p1
[17] Toba Y 1973 *J. Oceanogr. Soc. Jpn.* **29** 209
[18] Hwang P A, Wang D W, Walsh E J and Krabill W B 1984 *J. Phys. Oceanogr.* **30** 2753
[19] Brazhnikov M Y, Kolmakov G V and Levchenko A A 2002 *JETP Lett.* **95** 447
[20] Fal'kovich G E and Shafarenko A B 1988 *Sov. Phys. JETP* **67** 1393
[21] Wright W, Budakian R and Putterman S 1996 *Phys. Rev. Lett.* **76** 4528
[22] Wright W, Budakian R, Pine D and Putterman 1997 *Science* **278** 1609
[23] Henry E, Alstrom P and Levinsen M T 2000 *Europhys. Lett.* **52** 27
[24] Brazhnikov M Y, Kolmakov G V, Levchenko A A and Mezhov-Deglin L P 2000 *Europhys. Lett.* **58** 510
[25] Westra M T 2001 *Patterns and turbulence in surface waves* (Eindhoven: Technische Universiteit Eindhoven) p1
[26] Brazhnikov M Y, Kolmakov G V and Levchenko A A2000 *Europhys. Lett.* **58** 510
[27] Brazhnikov M Y, Levchenko A A, Kolmakov G V and Mezhov-Deglin L P 2001 *JETP Lett.* **73** 398
[28] Brazhnikov M Y, Levchenko A A, Kolmakov G V and Mezhov-Deglin L P 2001 *Low Temp. Phys.* **15** 229
[29] Peng H W, Yuan H J, Wang D J, Chen S Z and Lee C B submission to Phys. Fluids
[30] Packard N H, Crutchfield J P, Farmer J D and Shaw R S 1980 *Phys. Rev. Lett.* **45** 712
[31] Takens F 1981 *Dynamical Systems and Turbulence* (Berlin: Springer) p366
[32] Brandsater A and Swinney H L 1984 *Fluctuations and Sensitivity in Nonequilibrium Systems* (Berlin: Springer) p166
[33] Grassberger P and Procaccia I 1983 *Phys. Rev. Lett.* **50** 346
[34] Peng H W, Wang D J and Lee C B 2005 *Mod. Phys. Lett.* B **19** 1615
[35] Dias F and Kharif C 1999 *Annu. Rev. Fluid Mech.* **31** 301
[36] Huntley I 1977 *J. Fluid Mech.* **80** 81
[37] Wu J Z 1995 *Phys. Fluids* **7** 2357
[38] Lee C B 1998 *Phys. Lett.* A **247** 397
[39] Lee C B 2000 *Phys. Rev.* E **62** 3659
[40] Lee C B 2001 *Exp. Fluids* **30** 354